KAWASAKI STEEL TECHNICAL REPORT
No.45 (November 2001)
"Developed Machinery Maintenance Technology
in Steelmaking Plant"

Techniques for Long Life Materials Applied to Continuous Caster Roll

Satoh, Y.; Yamamura, T.; Takimoto, T.

Synopsis :
The purpose of caster roll investigations is to improve productivity and to contribute to energy and resouses saving by means of prolongation of caster roll lives. The experimental results show that thermal cracking is well correlated in terms of physical and mechanical properties of the rolls while steam oxidation is correlated with metallurgical structure at oxidation temperatures. The authors have successfully developed a heat resistant overlay alloy, "Super KBS", and a precipitation hardening overlay alloy, "W 630", for a caster roll equipped with no external cooling device and for that equipped with an external cooling device, respectivety. The two newly developed alloys have been applied to full-scale commercial caster rolls, consequently achieving the prolongation of caster roll lives.

The body can be viewed from the next page.

Techniques for Long Life Materials Applied to Continuous Caster Roll*


Yuji Satoh
Staff Deputy Manager, Equipment Technology Sec., Equipment Technology Dept., Chiba Works


Takashi Yamamura
Staff Assistant Manager, Equipment Technology Sec., Equipment Technology Dept., Mizushima Works


Takafumi Takimoto
General Manager, Equipment Technology Dept., Chiba Works

Synopsis:

The purpose of caster roll investigations is to improve productivity and to contribute to energy and resouses saving by means of prolongation of caster roll lives. The experimental results show that thermal cracking is well correlated in terms of physical and mechanical properties of the rolls while steam oxidation is correlated with metallurgical structure at oxidation temperatures. The authors have successfully developed a heat resistant overlay alloy, "Super KBS", and a precipitation hardening overlay alloy, "W 630", for a caster roll equipped with no external cooling device and for that equipped with an external cooling device, respectivety. The two newly developed alloys have been applied to full-scale commercial caster rolls, consequently achieving the prolongation of caster roll lives.

1 Introduction

Continuous caster rolls which are used for processing and transferring slabs during the solidification process repeatedly come into contact with solidifying slabs and cooling water. As a result, suffer the combined damage of thermal cracking and steam oxidation. The life of these rolls has an important effect on the productivity and maintenance costs of steel production facilities, therefore, a number of studies have been made from various aspects on these rolls.[1-4] Studies on the deterioration and damage mechanisms of these rolls have systematically and continuously been being advanced by Kawasaki Steel[5-7] and these studies have made it clear that what these rolls require are good thermal cracking and steam oxidation resistance properties.[7] Furthermore, we have found that thermal cracks propagate along expanding type prior-austenite boundaries in the middle of overlay welding beads and thermal cracks generated in reheat HAZ do not deeply propagate due to being bent to the direction of solidification from the radial direction of a roll because of the shape of the crystal grains extending in the direction of solidification together with the fine grain effect due to reheating.[5] We have also clarified that stable oxide layers are hardly ever formed in high temperature steam environments due to the outward diffusion of Ni.[6] This report explains the characteristics and performance of roll alloys for slow cooling and forced cooling which have been developed according to the research policies established on the basis of the knowledge and information mentioned above. Furthermore, this report includes the results of using these alloys in production facilities on an industrial scale.

2 Design Concept for Materials Strong Against the Application Environment

2.1 Slow Cooling Continuous Caster Roll Materials

In slow cooling continuous casters, although water-cooling is applied to the shaft of the rolls, the temperature on the outer surface becomes high because surface cooling results only from the splash of cooling water supplied to the slabs.

Therefore, what is required against thermal cracking is high temperature strength and it is necessary to strengthen the material by precipitation so that the strength is not deteriorated while in service. If the material is strengthened only by martensite strengthening, the effect is lost within a short period of time due to consol-

* Originally published in *Kawasaki Steel Giho*, 33(2001)1, 31-36

idation and collapse of laths.[7]

For protection against high temperature steam oxidation, on the other hand, in order to form oxide layers of Cr_2O_3, it is necessary to decrease the doping quantity of austenite formers which lower the Ac_1 transformation point.[8]

2.2 Forced Cooling Continuous Caster Roll Materials

In forced cooling of continuous casters, the rolls are provided with external cooling spray nozzles in addition to shaft water-cooling and the temperature at the roll surface is kept low. For these rolls, desirable alloys are those that can be easily strengthened by precipitation and have high strength below medium temperatures, or about 400°C from the thermal cracking resistance point of view. Furthermore, the alloys are required to have superior corrosion and steam oxidation resistance properties in the medium temperature range. From these points of view, precipitation hardened type stainless steel is suitable for forced cooling of continuous caster rolls and the important point becomes to improve toughness in the medium and high temperature range which is regarded as the weak point of these rolls.

3 Basic Characteristics of the Newly Developed Materials

3.1 Chemical Compositions and Production Methods

The standard compositions of conventional materials and the newly developed materials are shown in **Table 1** together with the welding methods. W 240 is an overlay material of 4Ni added 13Cr martensite stainless steel. This material became the primary choice by replacing the original Cr-Mo steel due to its high water corrosion and thermal cracking resistance properties. Super KBS was developed aiming at precipitation strengthening by increasing the carbon content and adding carbide formers. In consideration of the steam oxidation resistance performance, the Ni content was reduced and Co was doped because formation of δ-ferrite would be excessive if only the carbon content were increased. Here, Ni has a higher γ (austenite) formation performance than Cr and its diffusion speed in austenite is high, whereas, Co has a lower γ formation performance than Ni.

Table 1 Benchmark compositions of overlay materials

Name	Compositions (mass%)	Welding method	Remarks
W 240	0.08C-13.3Cr-4.0Ni	SAW (Band)	Conventional overlay
Super KBS	0.16C-12.9Cr-0.1Ni-Co, Mo, V, Cu	SAW (Band)	Developed overlay
W 630	0.04C-17.1Cr-4.5Ni-4.5Cu-0.12Nb	SAW (FCW)	Developed overlay

SAW: Submerged arc welding, Band: 50 mm wide strip welding, FCW: ϕ3.2 flux cored wire welding

25 μm

(a) W 240, PWHT 625°C × 4 h (b) Super KBS, PWHT 625°C × 4 h (c) W 630, PWHT 620°C × 4 h

Photo 1 Examples of microstructure of overlay materials

W 630 was developed following idea of development of 17-4 PH[9], by making use of martensite strengthening of the Cu-rich phase. The corrosion resistance property of this material is developed by the 17% Cr content and the 4.5% Ni doping. Continuous δ-ferrite can easily be formed because the Cr content is high. Furthermore, the Nb content was set at about 0.1% in order to prevent precipitation of the weakened phase[10] while aiming at improved strength.

Metal overlay welding is by the SAW (Band) method for W 240 and Super KBS and the SAW (FCW) method for W 630. The band method is superior in achieving uniformity of welding quality as well as in welding efficiency, however, it is difficult to apply this method to welding of metals containing many low melting point elements such as Cu because the molten pool is large resulting in generation of solidification cracking.

3.2 Metallurgical Structure

Microstructures of the conventional and newly developed materials are shown in **Photo 1**. Nitro-hydrochloric acid was used as the corrosion liquid. W 240 and Super KBS are of an annealed martensite (α') structure and a slight ferrite (α) structure is included. W 630 shows a $\alpha' + \gamma_R$ (retained austenite) structure. This structure is formed aiming at improving toughness. W 240 has slender martensite blocks and is assuredly of an expanding type prior-austenite structure grown in the direction of crystallization. In Super KBS, the blocks are cut into short pieces. The prior-austenite grains are fine[11] and the direction of crystallization is random.

Fine grain type martensite laths have been confirmed in TEM images and precipitation of minute $M_{23}C_6$ has been found at lath boundaries as well as in laths according to TEM-ED.[7] The α' part of W 630 is minute and TEM images have confirmed the precipitation of the Cu-rich phase in laths. Furthermore, precipitation is observed in γ_R grains.

3.3 Physical and Mechanical Properties at Room Temperatures

Various properties of each material are shown in

Table 2 Room temperature properties of overlay materials

Name	Ac_1 (°C)	α^* ($\times 10^{-6}$/°C)	λ (W/mK)	YS (MPa)	TS (MPa)	El (%)	RA (%)	Hardness (DPN)
W 240	555	11.5	21.3	721	825	17.5	58.0	283
Super KBS	650	10.9	25.3	925	1 122	12.5	33.5	361
W 630	620	11.9	17.1	734	989	14.8	33.7	329

α: Coefficient of expansion, α^*: R.T.~100°C, λ: Thermal conductivity

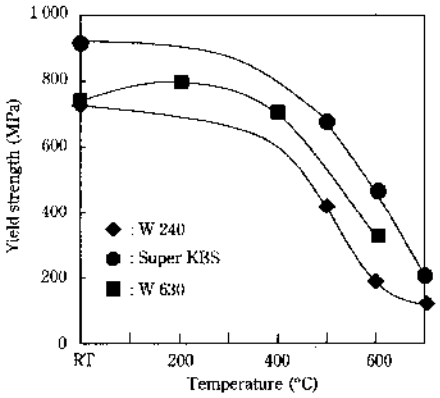

Fig. 1 Yield strength as a function of temperature

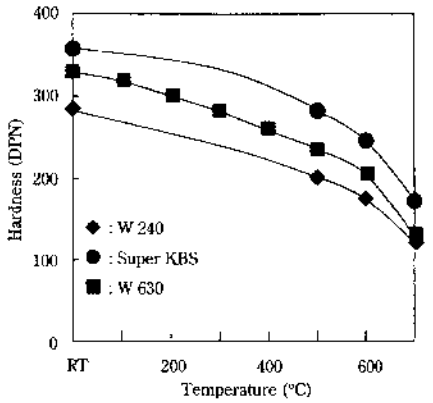

Fig. 3 Vickers hardness as a function of temperature

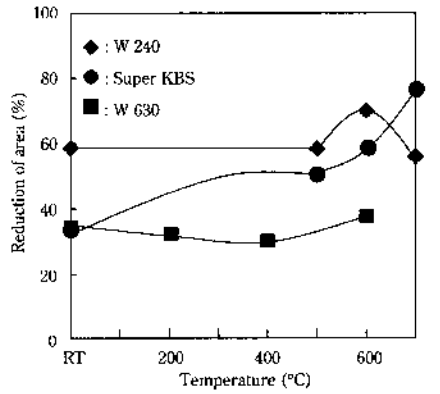

Fig. 2 Reduction of area as a function of temperature

Table 2. The Ac_1 transformation points shown are the transformation initiation temperatures. Super KBS has a high yield strength (YS) and a high thermal conductivity (λ) and its reduction of area is adequate. W 630 is of a $\alpha' + \gamma_R$ structure and the yield strength and hardness are both higher than those of W 240 which is mostly of a α' structure. This is caused by precipitation of the Cu-rich phase.

3.4 Mechanical Properties at High Temperatures

Continuous caster rolls are used at medium and high temperatures, therefore, the properties in this range of temperature are important. The yield strength, reduction of area and hardness are shown in **Figs. 1** to **3** respectively.

With respect to W 240 and Super KBS, which are used in slow cooling applications, the high temperature side properties were studied. For W 630, which on the other hand is used in forced cooling, the medium temperature properties were mainly investigated. Super KBS shows high yield strength and high hardness throughout the whole range of temperatures and its reduction of area also improves on the high temperature side. The strength of W 630 is equivalent with that of W 240 at room temperature, and exceeds it from the medium to high temperature ranges. Sharp decreases are not observed in the toughness even at medium to high temperatures.

4 Basic Properties of the Newly Developed Materials

4.1 Thermal Cracking Resistance Properties

4.1.1 Test method and conditions

Test pieces of $\phi 15 \times 5$ mm were taken from deposited metals. The pieces were heat cycled by raising the temperature using high frequency induction heating and then cooling by water spray. The length and numbers of cracks generated in these test pieces were then measured after completing the tests. With induction heating, the heated temperature of the actual test pieces varies depending on the magnetic permeability of the materials tested, therefore, thermocouples were fitted to the test pieces to measure the actual temperatures and the electric current and voltage were adjusted accord-

ingly. Due to the number of repetitions, the thermocouples eventually broke, and thereafter the temperature was maintained by controlling the current and voltage.

Two levels of test conditions were selected. The first level heating and cooling was between 20°C and 600°C and the second level was between 20°C and 700°C. The heating time and cooling time were set at 4 s and 3 s respectively and the number of cycles was 1 000. Optical microscopes were used for measuring the length and number of cracks.

4.1.2 Test results and examination

The test results are shown in **Fig. 4**. The maximum depth of the cracks generated in the test pieces (The maximum length of the cracks generated on the bottom surface of the test piece cylinders) is shown on the vertical axis using a logarithmic scale and the results for each material were plotted on the horizontal axis in the increasing order of yield strength at high temperatures from low to high.

In the lower temperature side test conditions, the maximum depth of the cracks decreases in the order of W 240, W 630 and Super KBS according to the high temperature yield strengths shown in Fig. 1. However, in the higher temperature side test conditions, the maximum depth is not correlated to the high temperature yield strength and the depth is the deepest with W 630.

Based on this observation, the thermal cracking resistance performance was evaluated using the formula proposed by K. K. Mehta et al.[12] which incorporates both the physical and mechanical properties of each alloy. The formula used is shown below.

$$P_{H/C} = \sigma_y \cdot \lambda / E \cdot \alpha \cdot c \cdot \rho \times 10^3 \cdots\cdots\cdots\cdots (1)$$

Where $P_{H/C}$: Thermal crack resistance parameter
σ_y: 0.2% yield strength (MPa)
λ: Thermal conductivity (W/mK)
E: Young's modulus (GPa)
α: Coefficient of thermal expansion (10^{-6}/°C)
c: Specific heat (J/kgK)
ρ: Density (g/cm^3)

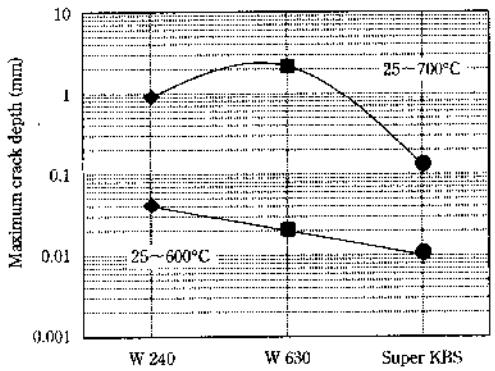

Fig. 4 Maximum crack depth of test pieces after thermal shock test (×1 000 cycles)

The test results orderly arranged using the thermal crack resistance parameter ($P_{H/C}$) are shown in **Fig. 5**. The result is the same even incorporating various properties of each alloy and correlation is observed in the lower temperature side test conditions, however, hardly any correlation can be observed in the higher temperature side test conditions.

Temperature holding was not included while heating test pieces in the heat cycle tests and the test pieces were cooled instantaneously, therefore, ordinary reverse transformation is unimaginable. However, it is conceivable that precipitation progressed due to the load of the heat cycles.

Therefore, the metallurgical structure of each material after the heat cycle tests was investigated. The microstructures at the tips of cracks after the tests on the higher temperature side are shown in **Photo 2**. The corrosion liquid used was nitrohydrochloric acid as in the examples shown in Photo 1.

Compared with Photo 1 taken before the heat cycle tests, W 240 in Photo 2 shows clear martensite blocks, presumably because precipitation progressed. The Super KBS surface shows that precipitation occurred at the prior-austenite boundaries and is separating the blocks.

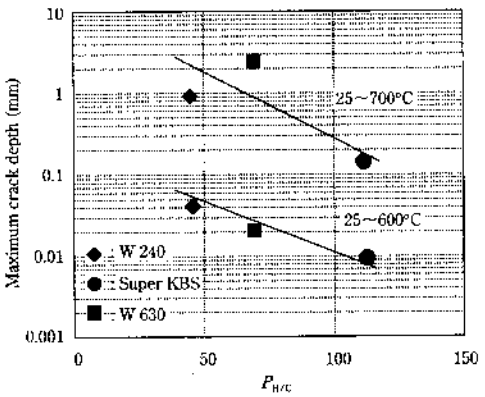

Fig. 5 Relation between maximum crack depth after thermal shock test and resistance against thermal shock parameter ($P_{H/C}$) at 600°C

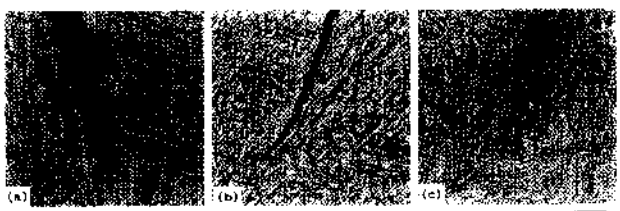

(a) W 240 (b) Super KBS (c) W 630

Photo 2 Microstructure of test pieces at the point of a crack after thermal shock test (×1 000 cycles)

Differently from the microstructure of W 240, the direction of the blocks is random; therefore, it is believed that the size of the prior-austenite grains is kept small.

The microstructure of W 630 changed during the heat cycle tests. Precipitation at boundaries increased, the minute α' structure observed in Photo 1 crumbled and precipitation in the γ_R structure cannot be observed either. The γ grains observed in this photograph expand along the direction of solidification. Cracks are propagating along γ grains and are terminating at γ crystal grain boundaries orthogonal to the direction of crack propagation.

As explained above, precipitation was advanced in each material and the mechanical properties were considered to have been changed from those obtained by high temperature tensile tests.

The form of precipitation is examined here. In W 630, MC carbide was precipitated at high temperatures, while in W 240 and Super KBS, $M_{23}C_6$ carbide was precipitated. Due to the difference in the number of atoms in a unit cell in these two cases, it is believed that MC carbide coagulates and softens in an early stage due to acceleration of precipitation caused by heat cycles and σ_y in Eq. (1) lowers in the precipitated regions.

Another point observed in the photographs of the microstructure after the heat cycle tests is the tip shape of cracks. The three pictures in Photo 2 are of the same magnification. However, when the tips of the cracks is compared, the width of those in W 240 is 3~6 time as wide as those in Super KBS and W 630 and it can be observed that the tips of the cracks lose sharpness due to steam oxidation during heat cycle testing. The extreme points are in the shape of an unfolded fan and are preventing the propagation of cracks.

From the above observation, it is presumed that thermal cracking is correlated to Eq. (1) as long as the material systems classified by phase transformation and precipitation are the same or the materials are in the temperature range where these materials exhibit equal behavior. Therefore, Super KBS has better performance than the conventional material W 240 throughout the entire range of temperatures tested and the same also applies to W 630 in the medium temperature range where correlation exists.

4.2 Steam Oxidation Resistance Properties

4.2.1 Test method and conditions

Test pieces of 2 mm × 20 mm × 20 mm taken from deposited metals were put in quartz tubes placed in a heating furnace and steam-saturated air of 500 ml/min was supplied at a pressure of 12.3 kPa. The steam-saturated air supplied was generated from distilled water in a flask placed in a thermostatic vessel. In order to catch oxides separated by oxidation, the test pieces were put on a quartz board. The dimensions and weights of the test pieces were measured beforehand using a micrometer and an electronic balance respectively and the test pieces were measured again by the electronic balance together with separated oxides after testing. As the unit evaluating weight gain due to oxidation, MDD ($mg \cdot dm^{-2} \cdot d^{-1}$) was used. As for the test conditions, the temperatures were 500, 600, 700 and 750°C and the holding time was 96 h at all temperatures.

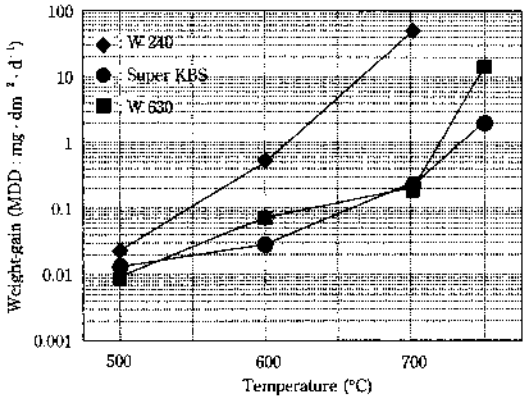

Fig. 6 Oxidation weight-gain exposed steam as a function of temperature

4.2.2 Test results and examination

The test results are shown in **Fig. 6**. Oxidation gain is plotted along the vertical axis on a logarithmic scale and the horizontal axis is the test temperature. Oxidation gain increases with temperature for every alloy. Both newly developed materials have better steam oxidation resistance properties throughout the entire temperature range than the conventional material. W 240 broke away at 700°C. Comparing the two new materials, oxidation gain is greater with Super KBS at 500°C and then with W 630 at 600°C, then at 700°C it is slightly greater with Super KBS and then switches back again to W 630 at 750°C. Severe internal oxidation occurs with W 630 at 750°C, therefore, it is presumed that no reversed phenomenon occurs at temperatures above 750°C.

With respect to the oxidation behavior of 18Cr steel and 18Cr-8Ni steel in high temperature steam, it has been reported that oxidation is greater with 18Cr steel at temperatures from 700°C to 800°C, and then reverses and becomes greater with 18Cr-8Ni steel between 900°C and 1 000°C.

What is conceivable from the above is that there are some changes in the microstructures. Therefore, the relationship between oxidation weight-gain and the Ac_1 transformation point was investigated. The transformation point considered here refers to the transformation initiation temperature.

The relationship between steam oxidation weight-gain and the Ac_1 transformation point of each alloy is shown in **Fig. 7**. In this figure, although some correlation can be observed at 600°C and 750°C, no correlation exists at 500°C and 700°C.

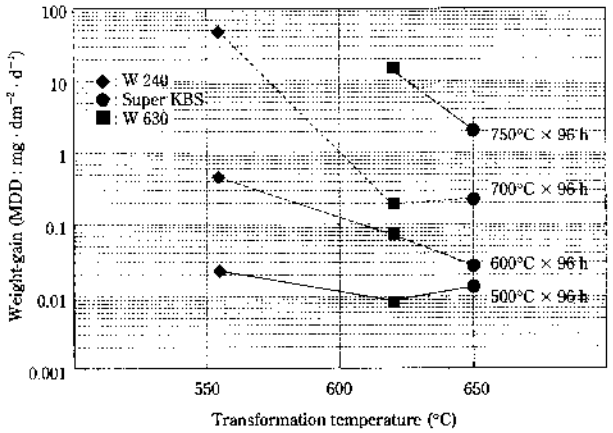

Fig. 7 Relation between oxidation weight-gain exposed steam and Ac_1 transformation temperature

(1) Steam Oxidation at 500°C

First of all, the phenomenon at 500°C is examined. It is presumed that at this temperature, the difference in diffusion speed of elements due to changes in the microstructure is not relevant because the temperature is below the transformation point for any one of these alloys and the differences in the surface oxidation film forming capacity of alloy elements has an effect on the oxidation weight-gain.

Therefore, the fact that oxidation weight-gain is more with W 240 than with Super KBS is believed to be because that although both alloys are of the $\alpha' + \alpha$ structure containing 13Cr, outward Ni diffusion occurs and stable formation of Cr_2O_3 is obstructed in W 240, which contains more Ni.[7] On the other hand, in W 630, the alloy contains 17%Cr, therefore, it is presumed that a stabilized oxide film of Cr_2O_3 is formed in the initial stage and outward Ni diffusion is less in this temperature range.

(2) Steam Oxidation at 600°C

The steam oxidation phenomena at 600°C are now considered. The surface layer microstructures after the tests at 600°C are shown in **Photo 3**. The corrosion liquid used was again nitro-hydrochloric acid. W 240 is in the process of $\gamma + M_{23}C_6$ transformation as the Ac_1 transformation point of 555°C is exceeded.

(a) W 240 (b) Super KBS (c) W630

Photo 3 Microstructure of test pieces at the outer layer after exposed steam test under a condition of 600°C × 96 h

Because abrupt contraction begins from 676°C, consolidation and collapse of martensite laths and formation of a decarbonized layer in the extreme outer layer occur in materials being held for a long time at this temperature.

In Super KBS, precipitation of carbides is observed in large quantities as the material is in the process of tempering in which discharge of carbon solid solution and precipitation of $M_{23}C_6$ are progressing.

W 630 is in a tempering process in which $\alpha + \gamma +$ Cu-rich phase transformation occurs and the minute α' (austenite) structure and precipitation observed in Photo 1 have become coarse. The microstructure existing here is considered to be of the $\alpha' + \alpha + \gamma_R +$ MC + Cu-rich phase because the temperature was below the Ac_1 transformation point of 620°C.

From the above-described observation and examination of the microstructures after the tests at 600°C, W 240 is of the $\alpha' + \alpha$ structure as at 500°C, however, the block unit has been coarsened. The diffusion speed is correlated to the temperature, therefore, it is presumed that when the temperature increases, outward diffusion of Fe and Ni which have a higher diffusion speed than Cr occurs preferentially, formation of minute Cr_2O_3, which is a stable oxide, is obstructed, inward diffusion of O is forced and steam oxidation progresses.[7]

Super KBS maintains a small block unit and, abrupt transformation and contraction to the $\gamma + M_{23}C_6$ structure start at 805°C. Although oxidation is accelerated at 600°C as compared with that at 500°C, outward diffusion of Fe is less with this alloy because of low Ni content.

On the other hand, W 630 is still in such a state at 600°C that formation of α (ferrite) structure is limited and resolution of γ_R (retained austenite) structure has not progressed either, therefore, it is believed that the diffusion speed of Fe and Ni in the γ (austenite) structure is fast and oxidation progresses more abruptly at 600°C than at 500°C. In other words, it is presumed that the phenomenon changes to-diffusion-controlled steam oxidation at this temperature although the Cr content in this alloy is more than that in Super KBS. The oxidation behavior of W 630 at 750°C is of the same behavior. However, γ_R at 600°C resolves at 750°C and the decrease in the diffusion speed of Cr and increase in the diffusion speed of Fe and Ni occur in the same way due to formation of reverse transformed γ.[14]

(3) Steam Oxidation at 700°C

As the next subject, various results of tests at 700°C are examined here. The results examined include such a phenomenon that once-progressed oxidation of W 630 was mitigated again. Due to the effect of the temperature rise from 500°C and 600°C, the oxidation curves of W 240 and Super KBS become steep. This is what is observed in ordinary phenomena of oxida-

tion in steam. However, the increase of oxidation is mitigated with W 630. In order to investigate this behavior, the microstructures after the test at 700°C were investigated.

In W 240, it is presumed that the microstructure was in the state of quenched α structure due to the reversely transformed γ being sharply cooled and because the block units are small, the microstructure had not reached the range of γ single phase and was in the range of $\gamma + M_{23}C_6$.

Super KBS is of the $\alpha' + \alpha$ structure. From the facts that coarsening of block units and carbides was observed and that the hardness curve at 700°C indicated a sharp drop, it can be presumed that coagulation of carbides occurred by steam oxidation in the case of this alloy.

The microstructure of W 630 as cooled after the test at 700°C is shown in **Photo 4**. By observing the microstructure, it can be seen that it is a mixed structure of quenched α' and α and a large amount of carbide is precipitated. However, γ_R cannot be found. In other words, these findings indicate that at this temperature, the $\alpha' + \gamma_R$ reversely transformed into $\gamma +$ MC through the process of γ_R being resolved into α + MC is being formed. It is presumed that the thus formed γ structure transformed into quenched α' through cooling after the test and the α structure remained as it was. Therefore, recovery of the steam oxidation resistance capacity due to the decrease of γ_R and increase of α occurs only at this temperature.

(4) Summary

From the above, it can be stated that steam oxidation is governed by the temperature and at temperatures below the Ac_1 transformation point, depends on the diffusion speed of the elements in the metallic crystal structures at the initial stage.

Therefore, in order to improve steam oxidation resistance performance at high temperatures, it is effective to raise the Ac_1 transformation point as observed with Super KBS.[8]

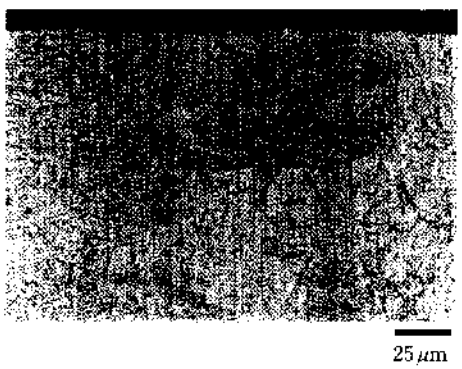

Photo 4 Michrostructure of test picec of material C at the outer layer after exposed steam test under a condition of 700°C × 96 h

Materials with their Cr content being increased as W630 show superior steam oxidation resistance performance by being used at temperatures in the medium range below 500°C even if the Ni content is high.

5 Evaluation in Production Facilities

The newly developed alloys were used on an industrial scale and their industrial cracking resistance performance was evaluated compared with those of the conventional material. **Figure 8** shows a comparison of the wear rations and **Fig. 9** shows a comparison of the depth of thermal cracking. The data on cracking of forced cooling continuous casters are the average of two values taken once each for two rollers once for an inner side roll and once for an outer side roll and the other data are values measured once. Both with slow cooling and forced cooling continuous casters, the wearing speed decreased to about one half and the thermal cracking depth decreased to less than one half. As for the difference due to the difference in part of using these alloys, the degree of damage is lighter when used on

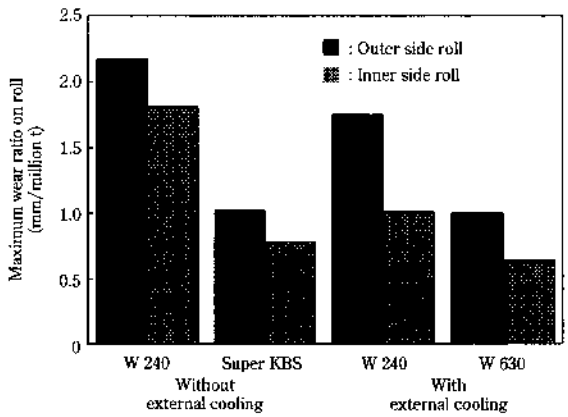

Fig. 8 Comparison of roll wear ratio

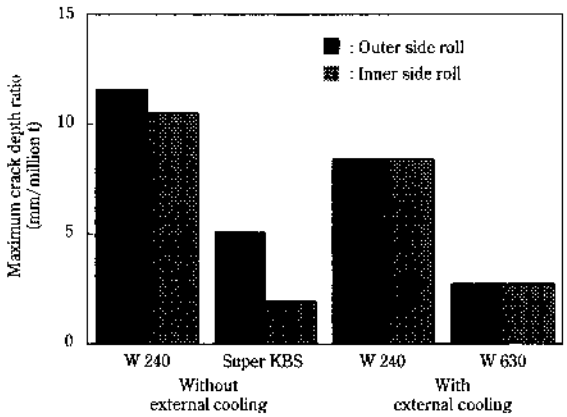

Fig. 9 Comparison of roll crack depth ratio

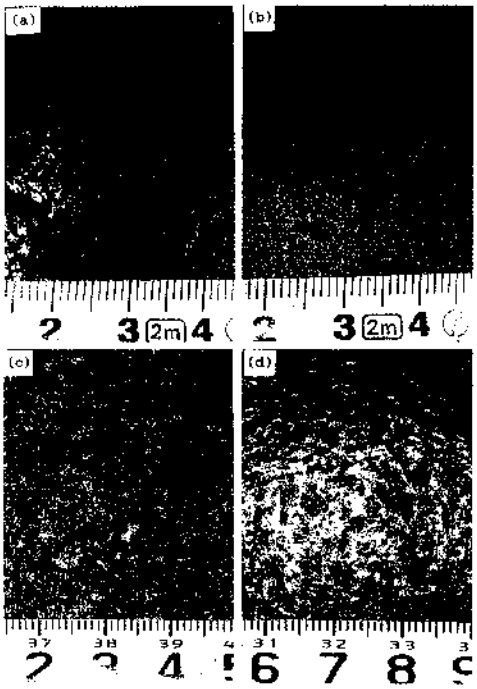

(a) W 240: after 1.45 million tons of production without external cooling
(b) Super KBS: after 1.45 million tons of production without external cooling
(c) W 240: after 1.48 million tons of production with external cooling
(d) W 630: after 2.50 million tons of production with external cooling

Photo 5 Appearance of outer side roll surface after application to commercial lines

inner side rolls than when used on outer side rolls. This is presumably because of the difference of whether cooling water was splashed or stably applied.

The surface appearance of the roll after use is shown in **Photo 5**. Photos (a) and (b) respectively show the surface appearance of the conventional material, W 240 and one of the newly developed materials, Super KBS, after using them for caster rolls for the same amount of production. The surface of Super KBS shows marked improvement both in the state of thermal cracking and oxidation film. Furthermore, with forced cooling continuous casters, W 630 still maintains its oxidation film even after being used for production of about 1.7 times that of W 240.

6 Conclusion

On the basis of the analysis results of the mechanism of deterioration and damages of the overlay welded metal of 13Cr-4Ni, which has been a primarily selected material, Super KBS, a slow cooling continuous caster roll material, and W 630, a forced cooling continuous caster roll material, have been developed. These roll materials replaced conventional materials and became primarily chosen materials in use in various environment and have been contributing to the stabilization and the improvement of continuous caster quality.

We hereby express our appreciation to Mr. Yukio Emoto of Tokushu Denkyoku Co., Ltd., for data on the mechanical properties and specimens for conducting metal structure tests, kindly provided in the process of developing W 630.

References

1) S. Kasai, Y. Satoh, A. Yanagisawa, A. Ichihara, and H. Ohnisi: *Kawasaki Steel Giho*, **19**(1987)1, 64
2) Y. Murai, S. Natsume, and S. Nishiyama: *Kobe Steel Eng. Rep.*, **40**(1990)3, 101
3) B. D. Horn: *Iron Steel Eng.*, (1996) July, 49
4) T. J. Nugent, T. J. Lonsbury, J. Didwall, and P. F. Schrof: *Iron Steel Eng.*, (1998) July, 52
5) Y. Satoh, T. Takimoto, A. Yokogawa, and T. Ishikawa: *CAMP-ISIJ*, **12**(1999)6, 1409
6) Y. Satoh, T. Takimoto, A. Yokogawa, and T. Ishikawa: *CAMP-ISIJ*, **12**(1999)6, 1410
7) Y. Satoh: 1st. Maintenance Gijutsu Zenkokutaikai, (2000)2, A-10, JIPM
8) Y. Satoh, K. Shinkawa, T. Takimoto, and Y. Kitani: *CAMP-ISIJ*, **9**(1996)4, 760
9) Y. Imai: *Kinzokugakkai kaiho*, **3**(1964)11, 581
10) M. Murayama, Y. Katayama, and K. Hono: *Met. Trans.*, **30**(1999) Feb., 345
11) Y. Satoh, I. Sanbonchiku, T. Nakada, and T. Takimoto: *CAMP-ISIJ*, **13**(2000)3, 561
12) K. K. Mehta, W. Schmid, and P. Schuler: Thyssen Edelst. Tech. Ber. Band, (1978) Heft 1, 34
13) W. H. Hatfield: *Iron Steel Inst.*, **115**(1927), 496
14) Y. Satoh, T. Nakada, and T. Takimoto: *CAMP-ISIJ*, **13**(2000)6, 1215